Electronic Supplementary Material (ESI) for Physical Chemistry Chemical Physics.

Electronic Supplementary Information: "Gas-phase Electronic Spectra of $HC_{2n+1}H^+$ (n=2–6) Chains"

Samuel J.P. Marlton, Chang Liu, Patrick Watkins, and Evan J. Bieske*

School of Chemistry, The University of Melbourne, Victoria, Australia 3010

E-mail: evanjb@unimelb.edu.au

Contents

S1 Calculated ground state vibrational frequencies

Table S1: Ground state vibrational frequencies for HC_5H^+ and HC_7H^+ calculated using CCSD/def2-SVP.

HC_5H^+			HC_7H^+		
mode	symmetry	frequency cm^{-1}	mode	symmetry	frequency cm^{-1}
ν_1	σ_g	3419	ν_1	σ_g	3442
ν_2	σ_g	2063	ν_2	σ_g	2151
ν_3	σ_g	781	ν_3	σ_g	1711
ν_4	σ_u	3414	ν_4	σ_g	568
ν_5	σ_u	1900	ν_5	σ_u	3442
ν_6	σ_u	1595	ν_6	σ_u	2098
ν_7	π_g	556	ν_7	σ_u	1764
ν_8	π_g	317	ν_8	σ_u	1091
ν_9	π_u	533	ν_9	π_g	640
ν_{10}	π_u	383	ν_{10}	π_g	461
ν_{11}	π_u	119	ν_{11}	π_g	127
			ν_{12}	π_u	628
			ν_{13}	π_u	498
			ν_{14}	π_u	296
			ν_{15}	π_u	95

Table S2: Ground state vibrational frequencies for HC_9H^+ and $HC_{11}H^+$ calculated using CCSD/def2-SVP.

HC_9H^+			$HC_{11}H^+$		
mode	symmetry	frequency cm^{-1}	mode	symmetry	frequency cm^{-1}
ν_1	σ_g	3458	ν_1	σ_g	3357
ν_2	σ_g	2179	ν_2	σ_g	2138
ν_3	σ_g	2105	ν_3	σ_g	2088
ν_4	σ_g	1261	ν_4	σ_g	1747
ν_5	σ_g	448	ν_5	σ_g	1057
ν_6	σ_u	3457	ν_6	σ_g	368
ν_7	σ_u	2161	ν_7	σ_u	3356
ν_8	σ_u	1767	ν_8	σ_u	2158
ν_9	σ_u	1599	ν_9	σ_u	2002
ν_{10}	σ_u	860	ν_{10}	σ_u	1872
ν_{11}	π_g	685	ν_{11}	σ_u	1376
ν_{12}	π_g	518	ν_{12}	σ_u	719
ν_{13}	π_g	314	ν_{13}	π_g	596
ν_{14}	π_g	68	ν_{14}	π_g	495
ν_{15}	π_u	693	ν_{15}	π_g	418
ν_{16}	π_u	492	ν_{16}	π_g	246
ν_{17}	π_u	405	ν_{17}	π_g	91
ν_{18}	π_u	183	ν_{18}	π_u	596
ν_{19}	π_u	29	ν_{19}	π_u	516
			ν_{20}	π_u	463
			ν_{21}	π_u	356
			ν_{22}	π_u	167
			ν_{23}	π_u	35

S2 Experimental band positions

Table S3: Band positions, widths, and assignments for REPD spectra of HC_5H^+ and HC_7H^+ chains.

cluster	λ_{air} nm	FWHM nm	wavenumber cm^{-1} (vac)	$\Delta\nu$ cm^{-1}	assignment
HC_5H^+	498.7±0.2	0.2	20048	-27	
	498.0±0.2	0.2	20075	0	$\tilde{A}^2\Pi_g \leftarrow \tilde{X}^2\Pi_u$
	487.8±0.2	0.2	20495	420	$2\nu_8$
	486.9±0.2	0.1	20532	457	$2\nu_{10}$
	456.2±0.2	0.1	21914	1839	ν_2
	447.7±0.2	0.2	22330	2255	$\nu_2 + 2\nu_8$
	447.0±0.2	0.2	22365	2290	$\nu_2 + 2\nu_{10}$
	421.0±0.2	0.1	23746	3671	$2\nu_2$
	361.2±0.3	0.6	27678	0	$\tilde{B}^2\Pi_g \leftarrow \tilde{X}^2\Pi_u$
	352.3±0.3	0.8	28377	699	ν_3
	338.4±0.3	0.4	29542	1864	ν_2
	330.6±0.3	0.4	30239	2561	$\nu_2 + \nu_3$
	327.1±0.3	0.5	30563	0	$\tilde{C}^2\Pi_g \leftarrow \tilde{X}^2\Pi_u$
	319.2±0.5	1.0	31319	756	ν_3
	308.3±0.8	1.2	32426	1863	ν_2
HC_7H^+	598.1±0.2	0.2	16714	-29	
	597.1±0.2	0.2	16743	0	$\tilde{A}^2\Pi_u \leftarrow \tilde{X}^2\Pi_g$
	533.6±0.2	0.2	18735	1992	ν_2
	484.9±0.2	0.1	20617	3874	$2\nu_2$
	482.5±0.2	0.1	20720	3977	
	447.0±0.8	0.8	22365	0	$\tilde{B}^2\Pi_u \leftarrow \tilde{X}^2\Pi_g$
	445.6±0.8	0.6	22435	69	
	436.0±0.8	1.2	22929	564	ν_4

Table S4: Band positions, widths, and assignments for REPD spectra of HC_9H^+, $HC_{11}H^+$ and $HC_{13}H^+$ chains. Band widths are upper limits except for the 545.1 nm and 542.3 nm transitions of $HC_{11}H^+$.

cluster	λ_{air} nm	FWHM nm	wavenumber cm^{-1} (vac)	$\Delta\nu$ cm^{-1}	assignment
HC_9H^+	695.5±0.2	0.3	14372	-27	
	694.3±0.3	0.3	14399	0	$\tilde{A}^2\Pi_g \leftarrow \tilde{X}^2\Pi_u$
	609.4±0.2	0.3	16405	2006	ν_2
	554.7±0.2	1.0	18023	3624	
	552.7±0.2	0.5	18088	3689	
	548.0±0.2	0.5	18243	3844	
	543.1±0.2	0.5	18408	4009	$2\nu_2$
	537.2±0.2	0.5	18610	4211	
	527.2±1.0	3.0	18963	0	$\tilde{B}^2\Pi_g \leftarrow \tilde{X}^2\Pi_u$
	478.5±0.5	2.0	20893	1930	ν_2
	475.7±0.5	2.0	21016	0	$\tilde{C}^2\Pi_g \leftarrow \tilde{X}^2\Pi_u$
	466.3±0.5	2.0	21439	423	ν_5
	436.2±1.0	1.0	22919	1903	ν_3
	433.0±2.0	2.0	23088	2072	ν_2
	425.5±2.0	2.0	23495	2479	$\nu_2 + \nu_5$
$HC_{11}H^+$	786.8±0.5	0.5	12709	0	$\tilde{A}^2\Pi_u \leftarrow \tilde{X}^2\Pi_g$
	682.2±0.5	0.3	14654	1945	ν_3
	679.3±0.5	0.3	14717	2008	ν_2
	621.5±0.5	0.4	16086		mixed
	620.7±0.5	0.4	16106		mixed
	619.2±0.5	0.4	16145		mixed
	613.1±0.5	0.4	16306		mixed
	611.5±0.5	0.4	16349		mixed
	606.2±0.5	0.4	16492		mixed
	602.3±0.5	0.4	16598		mixed
	596.6±0.5	0.4	16757		mixed
	545.1±0.3	1.5±0.5	18340	0	$\tilde{C}^2\Pi_u \leftarrow \tilde{X}^2\Pi_g$
	542.3±0.4	1.0±0.5	18435	95	mixed
	491.2±1.0	3.0	20352	2012	ν_2
$HC_{13}H^+$	873.8±0.6	0.8	11441	0	$\tilde{A}^2\Pi_g \leftarrow \tilde{X}^2\Pi_u$
	688.4±1.0	6.0	14522	0	$\tilde{B}^2\Pi_g \leftarrow \tilde{X}^2\Pi_u$
	606.0±1.0	4.0	16497	0	$\tilde{C}^2\Pi_g \leftarrow \tilde{X}^2\Pi_u$
	540.9±1.0	3.0	18483	1986	ν_4
	534.3±2.0	4.0	18711	2214	$\nu_4 + \nu_7$
	488.7±1.0	1.0	20457	3960	$2\nu_4$

S3 Spectra for $\tilde{A} \leftarrow \tilde{X}$ origin transitions for HC_5H^+, HC_7H^+, and HC_9H^+

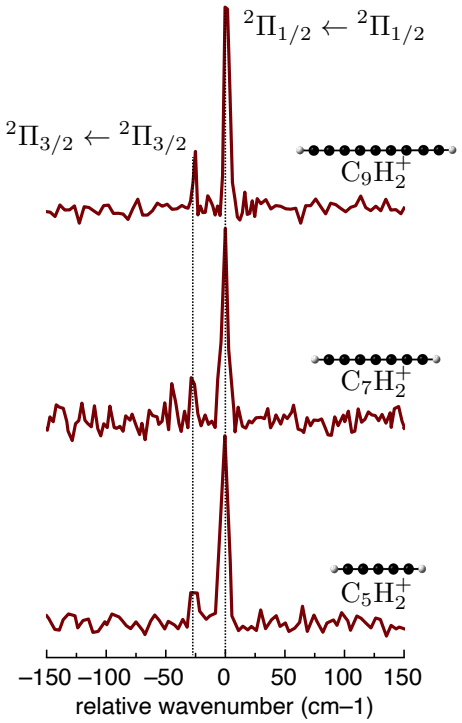

Figure S1: $\tilde{A}^2\Pi_{g/u} \leftarrow \tilde{X}^2\Pi_{g/u}$ origin transitions for HC_5H^+, HC_7H^+, and HC_9H^+. The weaker bands assigned to the $\tilde{A}^2\Pi_{3/2} \leftarrow \tilde{X}^2\Pi_{3/2}$ transition occur respectively 26 cm^{-1}, 29 cm^{-1}, and 27 cm^{-1} below the more intense $\tilde{A}^2\Pi_{1/2} \leftarrow \tilde{X}^2\Pi_{1/2}$ bands.

S4 Formation of $HC_{11}H^+$ from cyclic C_9^++HCCH

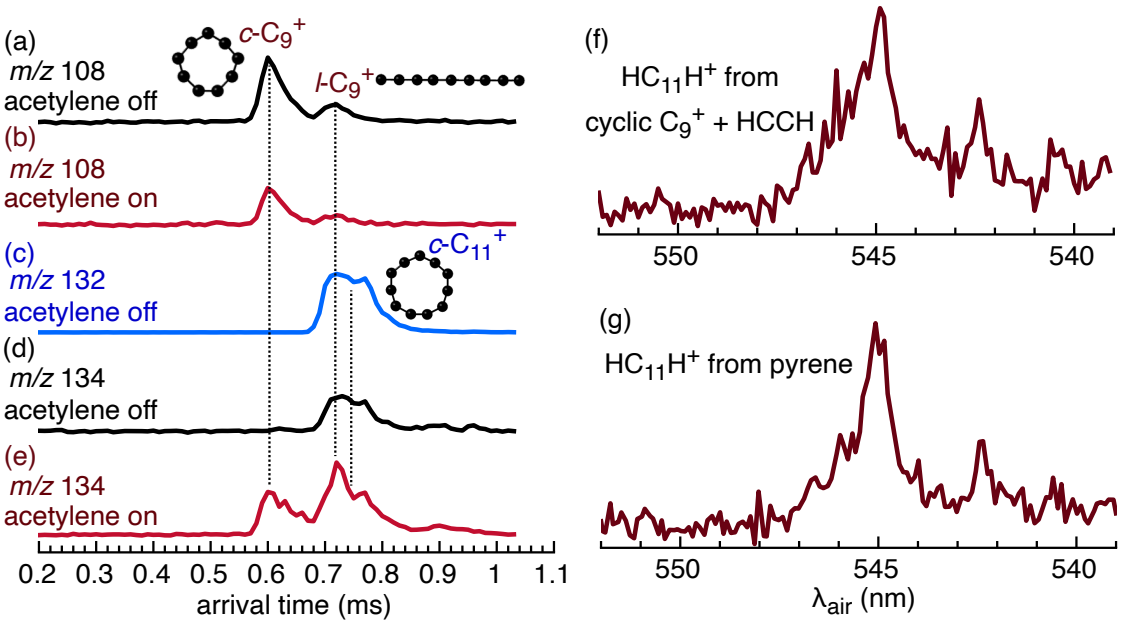

Figure S2: Ion mobility arrival time distributions selecting (a-b) m/z 108, (c) m/z 132, and (d-e) m/z134. For (b) and (e), the ions were reacted with acetylene for up to ≈500 ms after the ion mobility drift region in the hexapole ion guide. (f) REPD spectrum of m/z 134 ions formed by reacting mobility-selected c-C_9^+ ions with acetylene. (g) REPD spectrum of $HC_{11}H^+$ formed by photolysing pyrene with a pulses of 266 nm light.

Figures S2(a) and (b) show the arrival time distribution (ATD) for C_9^+ ions (m/z 108) without and with acetylene in the hexapole ion guide, respectively. The ATD for C_9^+ shows a peak for a cyclic isomer ($t_a \approx 0.60$ ms) and a linear isomer ($t_a \approx 0.72$ ms), both of which are depleted by reactions with acetylene. The arrival time distribution obtained by monitoring m/z 134 ions without acetylene in the hexapole is shown in Figure S2(d). Most of these m/z 134 ions are presumably C_{11}^+ containing two ^{13}C atoms, based on comparisons with the arrival time of m/z 132 C_{11}^+ (Figure S2(c)). When the carbon clusters are allowed to react with acetylene in the hexapole, there is a significant increase in the m/z 134 signal at the arrival time for cyclic C_9^+ indicating that cyclic C_9^+ reacted with acetylene to form $C_{11}H_2^+$ m/z 134 product ions.

To explore the nature of the $C_{11}H_2^+$ product ions, cyclic C_9^+ ions were isomer-selected using the ion-gate, and reacted with acetylene (see Figure 1(b)). The m/z 134 products were then mass-selected by the QMF and spectroscopically probed in the cryogenic ion-trap. The REPD spectrum of $HC_{11}H^+$ ions formed by reacting cyclic C_9^+ with acetylene (Figures S2(f)) is almost identical with the REPD spectrum of $HC_{11}H^+$ ions generated through the 266 nm photolysis of pyrene (Figure S2(g)), demonstrating that linear $HC_{11}H^+$ can be generated by bottom-up and top-down routes.

S5 Spectrum of $DC_{11}D^+$

$HC_{11}H^+$ is not the first hydrocarbon with an absorption band matching the λ5450 DIB. Previously, Linnartz *et al.* observed an absorption peak in an acetylene plasma using cavity ring down spectroscopy with position and width matching the λ5450 DIB,[1] The responsible species was later argued to be H_2CCC, leading to its assignment as the carrier of the λ5450 DIB,[2] an attribution that was later challenged.[3] To test whether the $HC_{11}H^+$ cation contributed to the 545 nm absorption observed by Linnartz *et al.* we measured the electronic spectra of $DC_{11}D^+$ formed from deuterated pyrene (Figure S3) finding that the $HC_{11}H^+$ band is blue-shifted by 0.3 nm upon deuteration, whereas the band reported in ref. 1 was shifted 1.5 nm to the red. Therefore, we conclude that the species formed in the acetylene plasma reported in ref. 1 is definitely not $HC_{11}H^+$.

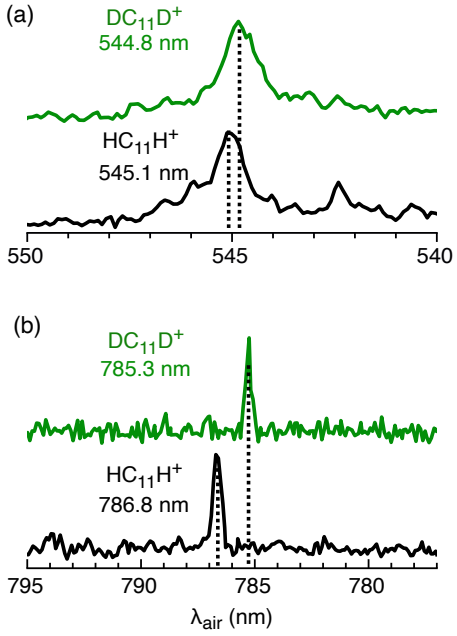

Figure S3: (a) $\tilde{C}^2\Pi_u \leftarrow \tilde{X}^2\Pi_g$ origin transitions for $DC_{11}D^+$ (upper) and $HC_{11}H^+$ (lower). (b) $\tilde{A}^2\Pi_u \leftarrow \tilde{X}^2\Pi_g$ origin transitions for $DC_{11}D^+$ (upper) and $HC_{11}H^+$ (lower). The HC_5H^+ and DC_5D^+ ions were generated from pyrene and deuterated pyrene, respectively.

S6 Comparison of weak $HC_{11}H^+$ bands and DIBs

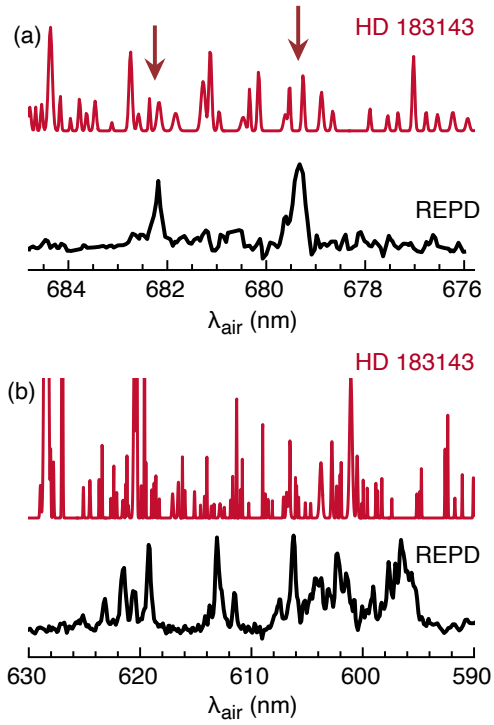

Figure S4: Laboratory REPD spectra of $HC_{11}H^+$ in the visible range. The spectra contain transitions to states with mixed $\tilde{A}$ and $\tilde{B}$ character. The REPD spectra are compared with synthetic astronomical DIB spectra for HD183143 generated using data from ref. 4. Arrows indicate DIBs close to the $HC_{11}H^+$ absorptions.

References

(1) Linnartz, H.; Wehres, N.; Van Winckel, H.; Walker, G.; Bohlender, D.; Tielens, A.; Motylewski, T.; Maier, J. A coincidence between a hydrocarbon plasma absorption spectrum and the λ5450 DIB. *Astron. Astrophys.* **2010**, *511*, L3.

(2) Maier, J.; Walker, G.; Bohlender, D.; Mazzotti, F.; Raghunandan, R.; Fulara, J.; Garkusha, I.; Nagy, A. Identification of H_2CCC as a diffuse interstellar band carrier. *Astrophys. J.* **2010**, *726*, 41.

(3) Krełowski, J.; Galazutdinov, G.; Kołos, R. Can H_2CCC be the carrier of broad diffuse bands? *Astrophys. J.* **2011**, *735*, 124.

(4) Hobbs, L. M.; York, D. G.; Thorburn, J. A.; Snow, T. P.; Bishof, M.; Friedman, S. D.; McCall, B. J.; Oka, T.; Rachford, B.; Sonnentrucker, P.; Welty, D. E. Studies of the diffuse interstellar bands. III. HD 183143. *Astrophys. J.* **2009**, *705*, 32.